Surfaces and Interfaces 28 (2022) 101683

Contents lists available at ScienceDirect

Surfaces and Interfaces

journal homepage: www.sciencedirect.com/journal/surfaces-and-interfaces

Effect of graphene oxide/hydroxyapatite nanocomposite on osteogenic differentiation and antimicrobial activity

Chingis Daulbayev [b,d,g], Fail Sultanov [a,b,d,*], Alina V. Korobeinyk [e], Mukhtar Yeleuov [b,c], Azamat Taurbekov [a,b], Baglan Bakbolat [b], Arman Umirzakov [c,d], Alzhan Baimenov [a,d], Olzhas Daulbayev [f,g]

[a] Al Farabi Kazakh National University, 172 Bogenbay batyr str, Almaty, Kazakhstan
[b] Institute of Combustion Problems, Almaty, Kazakhstan
[c] Satbayev Kazakh National University, Almaty, Kazakhstan
[d] National Laboratory Astana, Nazarbayev University, Nur-Sultan, Kazakhstan
[e] O.O. Chuiko Institute of Surface Chemistry of NAS of Ukraine, Kyiv, Ukraine
[f] Joint Institute for Nuclear Research, Dubna, Russian Federation
[g] Institute of Nuclear Physics, Almaty, Kazakhstan

ARTICLE INFO

Keywords:
Graphene oxide
Hydroxyapatite
Electrospinning
Antimicrobial activity
Osteogenic differentiation

ABSTRACT

This paper presents the fabrication and characterization of electrospun graphene oxide/calcium hydroxyapatite/polycaprolactone composite. Polycaprolactone is well-known for its excellent medical property and chemo-resistance. On the other hand graphene oxide (GO) and calcium hydroxyapatite (HAp) are both known for their superior biocompatibility, high mechanical properties, considerable electrical and thermal conductivity. Under current research GO and HAp were synthesized from an abundant bio-wastes material. As-prepared GO/HAp composite was dispersed in biodegradable polymer – polycaprolactone (PCL) in order to device a composite scaffold with the purpose to enhance osteogenic differentiation of osteoblasts for potential medical application. Synthesised composite was characterised using various chemo-physical methods. Biocompatibility was tested in the cell proliferation assay with preosteoblasts MC3T3-E1 cell line in order to identify any cytotoxic effect caused by its compounds. The bacteriostatic effect of GO was assessed using *Staphylococcus aureus* and *Escherichia coli* bacterial strains. Obtained GO/HAp/PCL composite scaffold can serve as a biologically compatible matrix for potential bone tissue regeneration with antimicrobial effect; provides an excellent biological compatibility for prospective application in medicine and clinical dentistry.

1. Introduction

Graphene oxide (GO) is widely used in various fields of science and technology due to it's unique mechanical and electrical properties [1]. A number of research groups have shown the prospects of GO application in nanoelectronics [2], biomedicine [3], as the main structural element for supercapacitors [4], fuel cells [5], as well as various types of sensors [6] and catalysts [7]. Wide application of GO is caused by its mechanical strength, high specific surface area, biological compatibility, high chemical and mechanical stability, which in turns facilitate synthesis of composite materials with enhanced properties. Over the past few years GO has been actively practiced in medical research in particular, for: targeted drugs delivery [8], tissue engineering [9], as antibacterial coatings [10], as an additive to improve mechanical properties and biocompatibility of medical substances. Calcium hydroxyapatite (HAp) a naturally occurring material and due to its excellent biological compatibility and osteoconductivity has long been used for bone regeneration, in the design of implants, and as an artificial bone tissue substitute. Despite exceptional biocompatibility the HAp has low mechanical stability, low specific surface area, low wear resistance, and low fracture toughness in comparison with the natural human bone tissue [11] which preclude its potential application in bone regeneration. To overcome these problems formulation of a composite scaffold structure based on GO/HAp dispersed in a polycaprolactone (PCL) matrix was proposed herein. Choice of PCL was made on a base of its high mechanical stability and biological compatibility, the resulting scaffold

* Corresponding author at: Al Farabi Kazakh National University, 172 Bogenbay batyr str, Almaty, Kazakhstan.
E-mail address: fail_23@bk.ru (F. Sultanov).

https://doi.org/10.1016/j.surfin.2021.101683
Received 7 September 2021; Received in revised form 11 December 2021; Accepted 12 December 2021
Available online 15 December 2021

can act as an osteoconductive framework that promotes the osteoblastic cells migration [12]. GO in the composite structure significantly improves the biological compatibility by the presence of many oxygen-containing groups, such as hydroxyl, epoxy, and carboxyl on its planes and edges. Moreover, it was reported that GO showed strong antibacterial activity [13]. However, the mechanism of its action on microbes is still not fully understood. Thus, the polymeric composite scaffold-like structure based on GO/HAp/PCL is one of the promising candidates for use in bone tissue engineering, combining together mechanical strength, biocompatibility, osteoconductivity and bacteriostatic properties.

To date, there are a number of established methods used for those composites fabrication such as plasma sintering [14], sol-gel method [15], biomimetic mineralization [16], as well as the electrospinning method [17]. Electrospinning, among all listed methods, has numerous advantages, which are: simplicity, appropriateness in GO/HAp composite scaffold engineering, as well as control on the forming polymer fiber diameters and the amounts of GO and HAp in the formed structure.

GO used in the work was obtained via carbonization and thermochemical activation of bio-waste material i.e., walnut shells. Although the resulting GO has a graphene-like structure, it has the mechanical, optical, and electrical properties comparable to pure GO. HAp for this research was synthesized via wet-chemistry route from recycled eggshells and phosphoric acid. The environmental sustainability of calcined calcium phosphates production from the milling of eggshell wastes and phosphoric acid is proven by abundance of eggshells as a byproduct of the household, hatcheries, bakeries restaurants and etc.; and potential environmental and health issues when those are dumped into landfill [18]. Diversion shell of eggs from the landfill to HAp is of high economic and environmental interest. Composites of GO/HAp dispersed in the PCL matrix, under current research, when cultured with MC3T3-E1 preosteoblasts had demonstrated the improved osteoblasts adhesion combined with strong antimicrobial effect. Antimicrobial properties of GO/HAp/PCL composite were studied against to *Staphylococcus aureus* and *Escherichia coli* bacterial strains in respect to the GO content.

2. Materials and methods

2.1. Reagents and materials

Phosphoric acid (H_3PO_4, 85%, Sigma Aldrich), eggshell (shells of chicken eggs, Almaty region, Kazakhstan), polycaprolactone (PCL, MW~1,300,000, Sigma Aldrich, USA), *Staphylococcus aureus* (*S. aureus*, ATCC®25,923, BioVitrum) and *Escherichia coli* (*E. coli*, ATCC®25,922, BioVitrum), MC3T3-E1 mouse preosteoblast cell line (provided by Kazakh National Medical University), α-minimum essential medium (α-MEM; Sigma Aldrich), fetal bovine serum (FBS; Sigma Aldrich), trypsin (E.C.3.4.4.4, 15,500 U/mg protein, Sigma Aldrich), phosphate-buffered saline (PBS, Sigma Aldrich), ethanol (C_2H_5OH, 90%, ChemPharm, Kazakhstan), nitric acid (HNO_3, 70%, Sigma Aldrich), urea (8 M (aq.), BioUltra), walnut shells (Almaty region, Kazakhstan), hydrochloric acid (HCl, 37%, Sigma Aldrich). All reagents were used without additional purification. Cell Counting Kit-8 (CCK-8) was purchased from Sigma-Aldrich and used according to manufacturers' instructions.

2.2. Methods

2.2.1. Synthesis of HAp

For the synthesis of HAp, the eggshells were preliminarily annealed at a temperature of 950 °C for 2 h in a muffle furnace (SNOL 30/1300) in an air medium with a heating rate of 30 °C/min. 1 g of CaO formed after thermal treatment of eggshells was mixed with an aqueous solution of orthophosphoric acid (6%, 20 ml) and stirred for 1 h on a magnetic stirrer at a speed of 100 rpm. The resulting solution was allowed to stand for 5 days; the solid deposit then was decanted and dried at the temperature of 100 °C for 4 h. The synthesized powder was post-thermally dehydroxylated in air medium at the temperature of 1200 °C for 2 h with a heating rate of 25 °C/min.

2.2.2. Synthesis of GO

Method for the graphene-like structures synthesis from walnut shells was described in detail in our previous works [19,20]. Graphene oxide was prepared from such graphene-like structures by means of chemical oxidation of as-obtained graphene-like structures. The mixture of nitric acid (35%) and urea (78 g/l) in the ratios 10:90, 20:80 and 30:70 was used as the oxidizing agent. Samples of a graphene-like structure were immersed into the oxidizer (in each experiment 2 g of graphene-like sample was dispersed in 100 ml of oxidized mixture) for 3 h under continuous stirring at 80 °C. Then the slurry was repeatedly washed with DI water in ultrasonic bath (32 kHz) until pH reached 4, then the solution was centrifuged and the carbonaceous powder was collected. The powder was further treated with 10% hydrochloric acid, washed with DI water until pH reached 3, and dried at 100 °C for 12 h.

2.2.3. Preparation of GO/HAp/PCL composite

To obtain composites based on GO, HAp and PCL, the electrospinning method was used. 0.5 g of PCL was dissolved in 10 ml of ethanol and GO and HAp were added to the mixture at certain ratios (Supplementary, Table 1) under constant stirring for 30 min on a magnetic stirrer at 120 rpm to ensure an even distribution of GO and HAp within the mixture. The resulting solution was loaded into a medical syringe (2.5 ml) and fibers were formed using the downward experimental setup (Supplementary, Fig. S.1).

2.3. Cytotoxicity assay

2.3.1. Cell cultures

MC3T3-E1 (passaese-16) was obtained from the Kazakh National Medical University then cultured in α-MEM supplemented with 10% FBS and 1% penicillin/streptomycin in an incubator (5% CO_2, 37 °C). The culture medium was refreshed every two days, and cells were passaged prior 100% confluence. At re-passaging cells were counted using the hemocytometer and a then cell suspension was plated onto tested samples in at a density of 2×10^4cells/cm^2 (24-well plate, Corning) and incubated as required.

2.3.2. Cell proliferation

Cell proliferation was investigated by Cell Counting Kit-8 (CCK-8), MC3T3-E1 used for seeding the surface were seeded in 24-well plate at a 2×10^4 cells/well at 37 °C with the addition of the tested samples (HAp, GO, GO/HAp/PCL composite) for 24 h. Prior to the experiment scaffold composite was powdered in order to unify experimental condition and simplify sample loading. Samples were sterilized via autoclaving, prior experiment and following concentrations: 50, 100, 150, 200, 250, 300, 350, 400, 450, 500 and 550 μg/ml; were used to test samples cytotoxicity, cells grown under medium were used as control. Three independent experiments were performed for each assay conditions. At 24 h after seeding, cell viability was measured using CCK-8. Further, according to the method described in [21–23], the cell proliferation profile was calculated

2.4. Antibacterial properties investigation

The antimicrobial activity of the composite samples against a representative Gram-positive bacteria *S. aureus* (ATCC 25,923) and a Gram-negative bacteria *E. coli* (ATCC 25,922) were assessed using the agar diffusion technique. Prior to the experiment samples were sterilized in autoclave. The agar diffusion assays were performed in 35 mm diameter Petri dishes containing Mueller-Hinton agar (Sigma-Aldrich) to a depth of 4 mm. The agar plates were spreaded with 100 μl 10^8CFU/ml of bacteria suspension prepared in sterile saline solution. A sterile tweezers was used to place 100 mg platelets of GO/HAp/PCL composite

with GO at different concentrations into each Petri dish. The agar surfaces were examined for possible clear halo appearance after incubation 24 h at 37 °C. Further, according to the method described in [10,24], the antibacterial activity of the samples was accessed. The presence of clarification that formed around sample platelets on the plate medium is recorded as inhibition against to bacteria strains tested. After incubation the diameter of inhibition zones were measured in millimeters to the nearest 0.1 mm using electronic calipers. Each experiment was repeated five times, mean and the standard deviations calculated; the antimicrobial index (AI) was expressed as (surface area of clear zone – surface area of sample) / (surface area of sample), and the surface areas were calculated using the ImageJ software.

2.5. Characterization of the obtained samples

Raman spectroscopy studies were carried out on the Raman spectrometer NTEGRA SPECTRA™ (NT-MDT Spectrum) equipped with solid-state laser at the excitation wavelength of 473 nm. FTIR spectra were recorded using a finely ground samples pressed in KBr pellets (pellets of 2 cm diameter were prepared by mixing of 3 mg sample with 300 mg KBr) in the wavenumber range of 4000–450 cm^{-1} at ambient temperature using FTIR spectrometer (Perkin Elmer, Spectrum 65). The structural features of the samples were analyzed with the transmission electron microscope (TEM, JEM-2100, Jeol, Japan). The surface morphology and elemental composition of the samples was examined by scanning electron microscope (SEM, Quanta 3D 200i, FEI, USA, at accelerating voltage of 15 kV) equipped with Oxford instrument X-sight EDX system. XRD spectra were recorded with X-Ray diffractometer (Drone-8, LOMO), using CuKa radiation (k = 0.15418 nm).

3. RESULTS and discussion

3.1. Characterization

IR spectra of the obtained biomass derived graphene-like material and GO are presented in Fig. 1b. The IR spectrum of graphene-like material is presented by two peaks with low intensity: 3430 cm^{-1}, corresponding to O-H stretching vibrations and the peak at 1620 cm^{-1}, which is assigned to the aromatic C-C stretching. After its chemical functionalization, the IR spectrum of the obtained GO is presented with peak at 3430 cm^{-1} with higher intensity, arising from the O-H stretching vibrations, peaks with low intensity at 2930 cm^{-1} and 2840 cm^{-1} attributed to sp^2 and sp^3 stretching bands of C-H, which are mainly caused by the defect sites of GO surface, the peak at 1620 cm^{-1}, which arises from the C-C aromatic stretching and the peak at 1260 cm^{-1} with highest intensity, corresponding to the C-OH stretching. Oxygen content in the GO structure was confirmed with EDX, and its amount ranges from 15.94 to 19.66% on the edges of GO sample (Supplementary, Fig. S.5), while the method does not detect oxygen in the middle parts of the GO sample.

Samples tested in current investigation has only a couple of Raman bands visible in the spectra (Fig. 1a), the in-phase vibration of graphene lattice (sp^2 characteristic or G band) at 1584 cm^{-1} as well as the disorder band (sp^3 characteristic or D band) caused by defective graphene structure at approximately 1357 cm^{-1}. The I_D/I_G ratios (defect ratio of graphene) are here obtained considering the peak intensity at D and G band frequencies. The graphene-like sample I_D/I_G value is equal to 0.81 confirming a highly defective structure associated with carbonization and thermo-chemical activation of biomass. However, both the G and D bands undergo significant transformation upon oxidation of graphene-like material. An observation is that oxidation leads to reduction in disorder band intensity (D band), as well as to appearance of 2D band at 2717 cm^{-1}. The I_D/I_G ratio of graphene oxide sample reduces to 0.36 compared to the one of graphene-like one. These results are in accordance with previously published reports [25–27]. Such transformation is presumably happened because oxidative mixture removes highly defected fragments from the sample to such extend that 2D band became well-resolved and helps to estimate the multilayer structure by I_{2D}/I_G ratio of 0.62 as a trilayer sample structure [28]. The relatively high intensity of D band in the graphene oxide after oxidative mixture treatment is probably due to the presence of unwashed amorphous carbonaceous agglomerates observed in TEM images (Fig. 2).

The TEM images are presented in Fig. 2, were used to characterize the surface morphology and structural features of GO. Morphology and topography of the obtained GO (Fig. 2) is typical of graphene materials. The high ordering and orientation of the carbon structure with the presence of transparent edges, according to [29], indicates a small thickness of the material [30], confirming three-layer structure of graphene oxide sample concluded from Raman spectroscopy. TEM images (Fig. 2) shows agglomerates of amorphous carbon (with an average diameter of 18.5 nm) entrapped into the sample structure and unwashed with oxidative treatment.

The characterization of the synthesized HAp powder was performed using XRD (Fig. 3a) and SEM (Fig. 3b) analysis. XRD spectra of synthesized HAp (Fig. 3, a) completely coincide with the JCPDS card no. 09–0432 of hydroxyapatite and the average crystallite size was calculated from the broadening in the XRD pattern according to Scherrer's equation as 17.1 nm. The values of the lattice parameters are also in agreement with the data obtained in [31–33] and are the following: a= 9.8218 ± 0.004; b= 2a; c= 9.473 ± 0.002, which is of hexagonal lattice

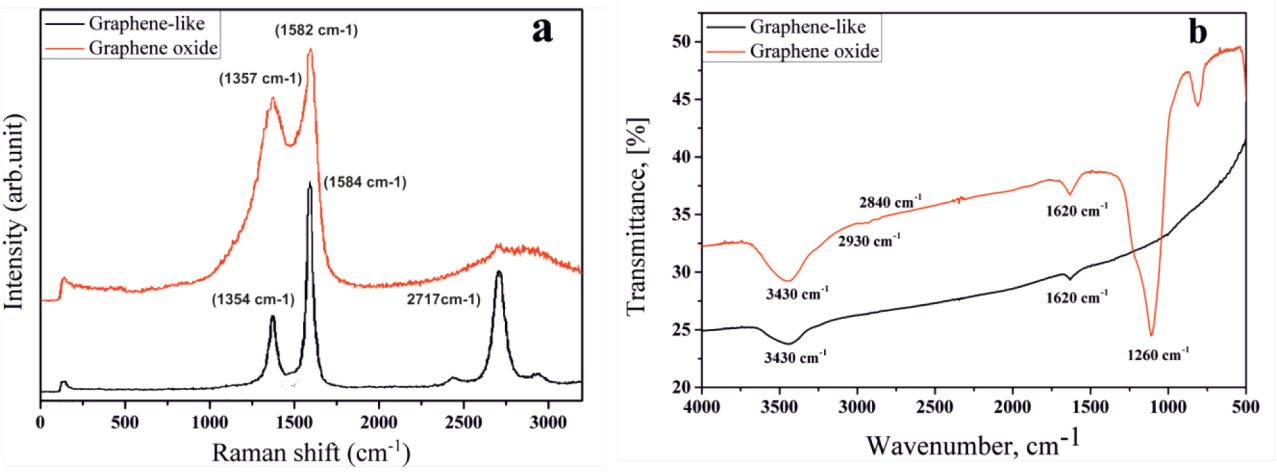

Fig. 1. Evolution of Raman spectra during the oxidation of graphene-like structure into graphene oxide (a) and IR spectra (b) of graphene-like structure and graphene oxide.

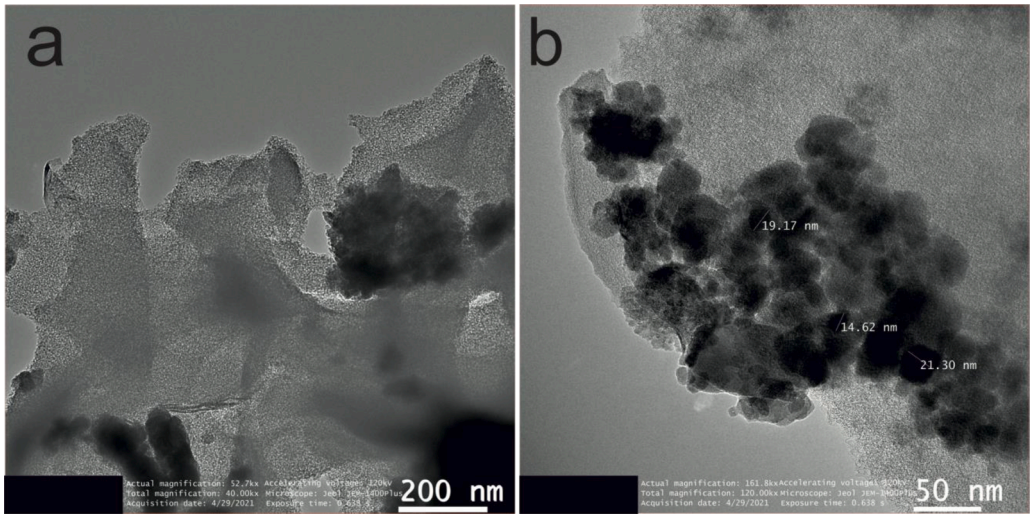

Fig. 2. TEM images of synthesized GO (TEM image of extended area of Graphene oxide sample (a) and a "zoom-in" counterparts of sample (b)).

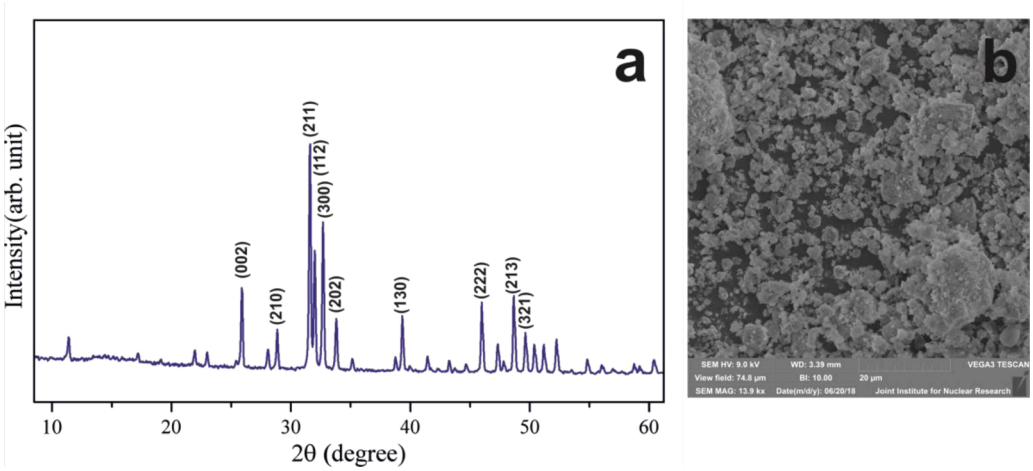

Fig. 3. XRD spectra (a) and SEM (b) image of as-synthesized HAp.

structure. SEM images of as-obtained HAp sample revealed average agglomerate diameters of about 10 μm. However, within the composite scaffold structure only particles of Hap with sizes less than 100 nm were detected (Fig. 4), This can be explained by the size reduction of HAp particles under high voltage at the time of electrospinning [34–36]. An apparent reason for such particle refinement this is the effect of an electric field, which concentrates inside of solid dielectric, resulting in the large HAp particles destruction. Chemical composition of the HAp was determined using EDX (Supplementary, Fig. S.4).

Fig. 4 captures SEM images of the resulting composite morphology in the form of a typical filamentous polymer fibers with the GO and HAp inclusion. The conducted semi-quantitative analysis indicates the presence of HAp particles in the structure of polymer fibers (Supplementary, Figs. S.2 and 3), and simultaneously, according to [37], rough spots on SEM images (Fig. 4, c and d) indicate the presence of GO in the structure of the formed fibers. Presence of oval shaped formations in SEM (Fig. 4, a and b) is attributed to the HAp inclusion into the structure of electrospun layer (confirmed by EDX, Supplementary, Figs. S.2 and 3) and described in literature for similar systems [38].

3.2. Antibacterial activity evaluation

Qualitative results of antimicrobial activity of composites in the presence of bacteria strains of *S. aureus* and *E. coli* are shown in Fig. 5. All tested composites showed an inhibition zone with the absence of microorganism growth, confirming the antibacterial activity (Table 1). Sample of GO/HAp/PCL (0.1 wt.% of GO) yielded the larger clear zone on both strains (AI are 9.59 and 6.53 for *E. coli* and *S. aureus*, correspondingly), whereas lower GO loading in GO/HAp/PCL (0.05 wt.% of GO) sample resulting in decreasing of the clear zone diameters strains (AI are 4.58 and 2.13 for *E. coli* and *S. aureus*, correspondingly).

Presence of GO in the composite structure greatly depresses the bacteria growth (Table 1, Fig. 5). Analysis revealed that the composite disregards to the GO concentration has more pronounced inhibitory effect against the Gram-negative bacteria *E. coli* compared to the Gram-positive bacteria *S. aureus*.

Several studies [39,40] devoted to the use of graphene and graphene-based structures in medicine made an assumptions about the mechanisms of the antimicrobial effect of GO. Such as authors [41] considered that GO is prone to the reactive oxygen species (ROS) and free radical (FR) formation which prevents the microbial growth. The obtained results, demonstrate the effect of GO on the antibacterial properties of composite structure, in some cases exceeding 97% (Fig. 5). This remarkable effect of GO can be explained not solely by ROS or FR but as well might be associated with sharp edges and the high level of fictionalization, which in turn damage physically membranes of bacterial cells. Evaluation of the antibacterial properties of the obtained composite structures showed a significant increase in the diameter of the

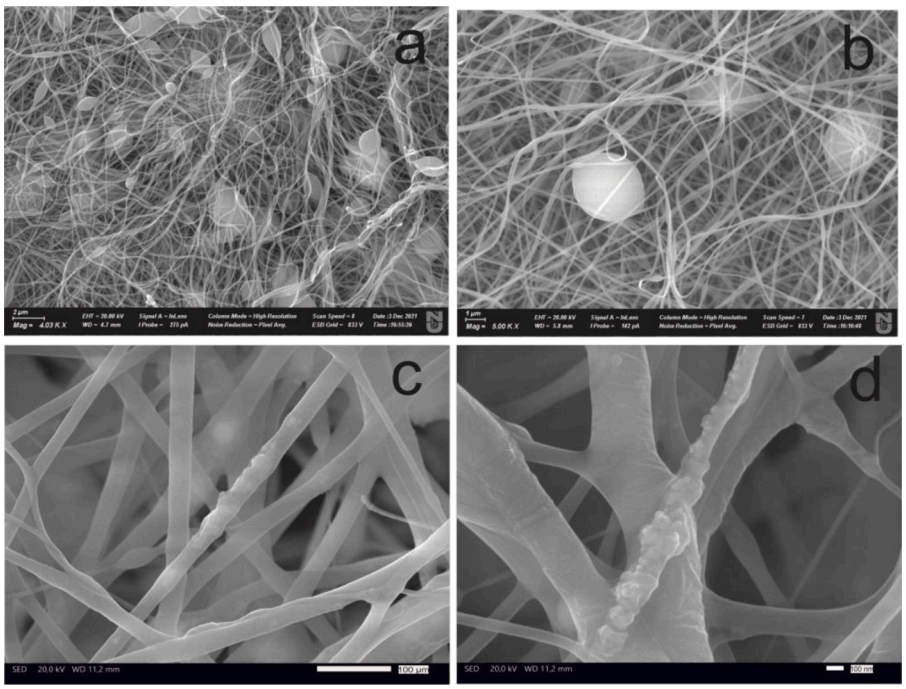

Fig. 4. "Zoom-in" SEM images of GO/HAp/PCL composite counterparts. Scale bars: 2 μm (a), 1 μm (b), 100 μm (c) and 100 nm (d).

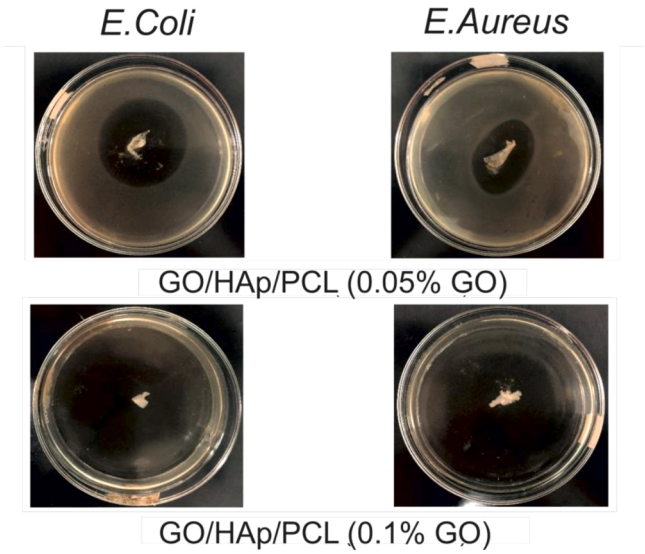

Fig. 5. Digital images of antibacterial activity tests for GO/HAp/PCL composite with different GO loading towards *E. coli* and *S. aureus*.

zone of inhibition (Fig. 5) from 5.2 to 9.1 mm with an increase in the GO content in the composite based on GO/HAp/PCL from 0.05 up to 0.1 wt. %. The obtained experimental results are in agreement with the works [42–44] and confirm the excellent antibacterial properties of graphene containing composite tested under current investigation.

3.3. Cytotoxicity of GO/HAp/PCL composites

Cell survival under the influence of HAp, GO and a composite GO/HAp/PCL (Fig. 6) decreases with an increase in their concentration in the solution. For a HAp concentration of 350 μg/ml, cell viability decreased to 57%, which is associated with a change in the pH of the medium upon the addition of HAp, leading to a sharp decrease in cell proliferation. It was shown in [45,46] that despite the fact that the size

Table 1
Antimicrobial activity of GO/HAp/PCL composite against to *E. coli* and *S. aureus* in respect to the GO loading.

Microorganisms	Zone of inhibition (mm)		Antimicrobial index	
	GO/HAp/PCL_0.05[a]	GO/HAp/PCL_0.1	GO/HAp/PCL_0.05	GO/HAp/PCL_0.1
Gram-positive bacteria				
Staphylococcus aureus	7.21 ± 0.55[b]	19.32 ± 0.92	2.13	6.53
Gram-negative bacteria				
Escherichia coli	16.87 ± 0.62	26.2 ± 1.01	4.58	9.59

[a] Concentration of GO in the composite.
[b] Values of zone inhibition are represented as mean ± standard deviation.

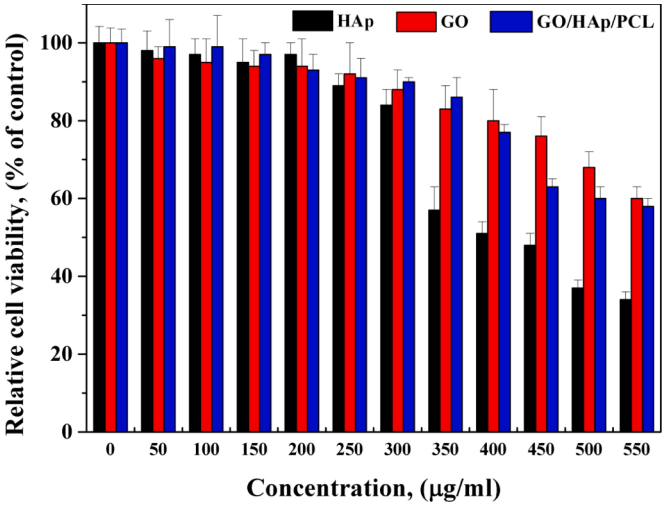

Fig. 6. *In vitro* cytotoxicity investigations of GO, HAp and GO/HAp/PCL samples in respect to their concentration.

and shape of HAp particles significantly affect cytotoxicity, they can be used as bone grafts. In turn, the cell viability for the GO/HAp/PCL composite (Fig. 6) shows that for concentrations up to 250 μg/ml composite has no statistically significant cytotoxicity, and even at limit concentrations of 550 mg/ml its effect is much lower than that of Hap at 350 μg/ml. In current experiment viability of MC3T3-E1 is higher on a GO sample and statistically equal to that one for GO/HAp/PCL composite at highest concentrations (500 and 550 μg/ml). Data for the GO/HAp/PCL sample indicates negligible cytotoxicity in concentration range from 50 to 350 μg/ml. The further increase in sample concentration gradually decreases cells viability mainly due to the HAp presence in the sample structure. Thus, the positive effect of GO in a composite structure with HAp on the viability of MC3T3-E1 preosteoblasts was reported due to the ability of graphene nanosheets to sequestrate [47]. In addition, it is proposed that GO in the structure of the GO/HAp/PCL composite binds HAp particles, which significantly affects cytotoxicity of the cells. utilization of polymer scaffolds reinforced with diverse materials such as graphene (GO), carbon nanotubes, as well as biocompatible materials, is of great interest in tissue engineering. These composite scaffolds can be used as an extracellular matrix, providing not only mechanical support for cells, but also effectively influencing the migration of both nutrients and individual components. Further, the introduction of GO in the structure of such composite impart the antibacterial properties to the resulting material. Existing models describes the effect of GO on bacteria indicate the high demand in more detailed both *in vivo* and *in vitro* study, for a deeper understanding of the influence of various factors, including synthetic approach and source of GO, HAp and the resulting composite, as well as biological compatibility and degradation rate of the polymer matrix.

GO has the highest antibacterial activity among carbon-containing materials [41], which is explained by the high specific surface area, which provides high adsorption activity. In addition, the local defects in the GO's sheet cause mechanical destruction of bacterial cell via direct interaction (Fig. 7). At the same time, authors [48–50] indicates the cytotoxic effect ROS and FR on bacteria. The performed studies are in agreement with pioneering works in the field of studying the mechanism of bacterial inactivation by creating composites based on GO, rGO, and graphene. Presumably, the basis of this mechanism lies in the mechanical effect of a defective structure on cell membranes, thereby causing their destruction and death. This effect on bacteria is also observed for other carbon materials such as carbon nanotubes, graphite and amorphous carbon. Despite the fact that the mechanism of GO antibacterial activity is extremely complex and the described pathways of action on bacterial membranes are not fully understood, it can be assumed that GO sheet structural defects, the number of layers, and functional groups create the bacterial membrane destruction. It is proposed that GO obtained from bio-wastes with great number of structural defects, great deal of fictionalization and with residual amounts of other carbon structures has an advantage over commercial GO due to abundant source material, and imperfections which impart the antimicrobial activity. The complex composite polymer matrices containing GO and HAp are successfully utilized as biologically compatible scaffolds that can be applied as an extracellular matrix, providing mechanical support, cell growth, and nutrient transport.

4. Conclusion

GO and HAp were syntesised under current investigation from abundant bio waste materials. Furthermore, polycaprolactone solution was used as a binder and composites of (GO/HAp/PCL) were successfully manufactured via the electrospinning method. The resulting structures were studied using a variety of analytical research methods, including XRD, TEM, SEM, Raman and IR spectroscopy. Comprehensive analysis showed that the synthesized HAp has a purity of over 97%, and the parameters of its crystal lattice completely coincide with biological apatite. Based on the obtained results, it was suggested that GO obtained from biomass (walnut shells) with carbon-containing impurities, such as amorphous carbon and graphene, not only possesses antibacterial activity, but is also more economically advantageous compared to pure commercial GO. This can be explained by the fact that the presence of defective structures and carbon-containing impurities increases the destruction on bacteria and leads to their mechanical damage. Composites, studied under current investigation shown great antimicrobial activity against to Gram-positive and Gram-negative bacteria strain in respect to the GO loading. Also, studied GO/HAp/PCL composite have no cytotoxic effect towards the MC3T3-E1 preosteoblast cells, and the observed decrease in cell proliferation is related to high sample loading (350 mg/ml and higher). Both GO and GO-loaded composite shown good biocompatibility which indicates a positive effect of GO in a composite structure with HAp on a PCL matrix on cell attachment, proliferation and possible further differentiation.

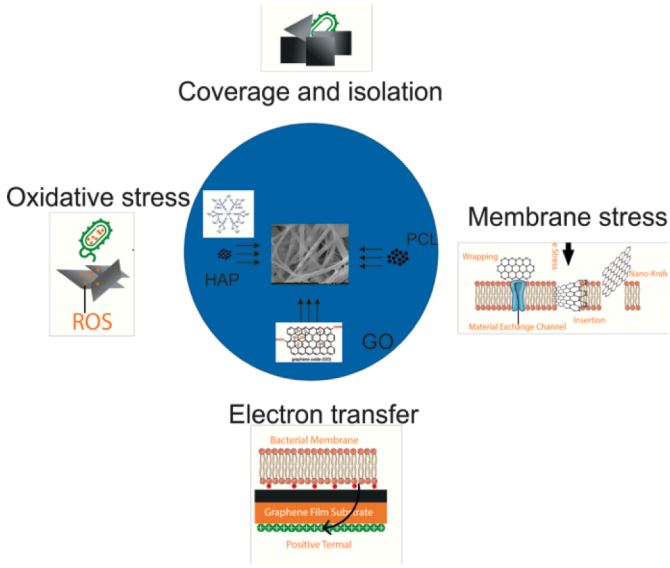

Fig. 7. Schematic illustration of the mechanisms of the antibacterial effect of GO.

CRediT authorship contribution statement

Chingis Daulbayev: Conceptualization, Writing – original draft. **Fail Sultanov:** Project administration, Writing – original draft. **Alina V. Korobeinyk:** Methodology. **Mukhtar Yeleuov:** Methodology. **Azamat Taurbekov:** Investigation, Writing – review & editing. **Baglan Bakbolat:** Investigation, Writing – review & editing. **Arman Umirzakov:** Investigation, Writing – review & editing. **Alzhan Baimenov:** Resources, Formal analysis. **Olzhas Daulbayev:** Resources, Formal analysis.

Declaration of Competing Interest

The authors declare that they have no known competing financial interests or personal relationships that could have appeared to influence the work reported in this paper.

Acknowledgments

This research is funded by the Science Committee of the Ministry of Education and Science of the Republic of Kazakhstan (Grant No AP09561955).

Supplementary materials

Supplementary material associated with this article can be found, in

the online version, at doi:10.1016/j.surfin.2021.101683.

Reference

[1] S.S.A. Kumar, S. Bashir, K. Ramesh, S. Ramesh, New perspectives on graphene/graphene oxide based polymer nanocomposites for corrosion applications: the relevance of the graphene/polymer barrier coatings, Prog. Org. Coat. 154 (2021), 106215, https://doi.org/10.1016/j.porgcoat.2021.106215.

[2] C. Lu, X. Wang, X. Zhang, H. Peng, Y. Zhang, G. Wang, Z. Wang, G. Cao, N. Umirov, Z. Bakenov, Effect of graphene nanosheets on electrochemical performance of Li 4 Ti 5 O 12 in lithium-ion capacitors, Ceram. Int. 43 (2017) 6554–6562, https://doi.org/10.1016/j.ceramint.2017.02.083.

[3] I. Prattis, E. Hui, P. Gubeljak, G.S. Kaminski Schierle, A. Lombardo, L.G. Occhipinti, Graphene for biosensing applications in point-of-care testing, Trends Biotechnol. (2021), S0167779921000111, https://doi.org/10.1016/j.tibtech.2021.01.005.

[4] B. Balli, A. Şavk, F. Şen, Graphene and polymer composites for supercapacitor applications, in: nanocarbon and Its Composites, Elsevier (2019) 123–151, https://doi.org/10.1016/B978-0-08-102509-3.00005-5.

[5] A. Alaswad, T. Wilberforce, A. Baroutaji, A.G. Olabi, Graphene based materials for supercapacitors and fuel cells. Reference Module in Materials Science and Materials Engineering, Elsevier, 2021, https://doi.org/10.1016/B978-0-12-815732-9.00063-2. B9780128157329000000.

[6] M.M. Ruiz-Ramirez, C. Silva-Carrillo, J.J. Hinostroza-Mojarro, Y.Y. Rivera-Lugo, P. Valle-Trujillo, B. Trujillo-Navarrete, Electrochemical sensor for determination of nitrobenzene in aqueous solution based on nanostructures of TiO_2/GO, Fuel 283 (2021), 119326, https://doi.org/10.1016/j.fuel.2020.119326.

[7] H.C.L. Geraldino, T.K.F.S. Freitas, D.D. Manholer, F. França, J.H. Oliveira, E. A. Volnistem, A.R.F. Lima, M. Bertotti, E.M. Girotto, J.C. Garcia, Electrochemical generation of H_2O_2 using gas diffusion electrode improved with rGO intensified with the Fe_3O_4/GO catalyst for degradation of textile wastewater, J. Water Process Eng. 36 (2020), 101377, https://doi.org/10.1016/j.jwpe.2020.101377.

[8] A. Ghamkhari, S. Abbaspour-Ravasjani, M. Talebi, H. Hamishehkar, M.R. Hamblin, Development of a graphene oxide-poly lactide nanocomposite as a smart drug delivery system, Int. J. Biol. Macromol. 169 (2021) 521–531, https://doi.org/10.1016/j.ijbiomac.2020.12.084.

[9] M.E. Berrio, A. Oñate, A. Salas, K. Fernández, M.F. Meléndrez, Synthesis and applications of graphene oxide aerogels in bone tissue regeneration: a review, Mater. Today Chem. 20 (2021), 100422, https://doi.org/10.1016/j.mtchem.2021.100422.

[10] X. Song, L. Xie, M. Zhang, W. Wang, L. Li, X. Lu, P. Lei, D. Liu, Y. Chen, H. Chen, C. Zhao, Cu-decorated graphene oxide coatings with enhanced antibacterial activity for surface modification of implant, Mater. Res. Bull. 141 (2021), 111345, https://doi.org/10.1016/j.materresbull.2021.111345.

[11] A. Bensalem, O.K. Kucukosman, J. Raszkiewicz, F. Topkaya, Synthesis, characterization, bactericidal activity, and mechanical properties of hydroxyapatite nano powders impregnated with silver and zinc oxide nanoparticles (Ag-ZnO-Hap), Ceram. Int. (2021), https://doi.org/10.1016/j.ceramint.2021.04.139. S0272884221011834.

[12] A. Shapourzadeh, S.M. Atyabi, S. Irani, H. Bakhshi, Osteoinductivity of polycaprolactone nanofibers grafted functionalized with carboxymethyl chitosan: synergic effect of β-carotene and electromagnetic field, Int. J. Biol. Macromol. 150 (2020) 152–160, https://doi.org/10.1016/j.ijbiomac.2020.02.036.

[13] M. Azizi-Lalabadi, H. Hashemi, J. Feng, S.M. Jafari, Carbon nanomaterials against pathogens; the antimicrobial activity of carbon nanotubes, graphene/graphene oxide, fullerenes, and their nanocomposites, Adv. Colloid Interface Sci. 284 (2020), 102250, https://doi.org/10.1016/j.cis.2020.102250.

[14] M.Z.I. Nizami, S. Takashiba, Y. Nishina, Graphene oxide: a new direction in dentistry, Appl. Mater. Today 19 (2020), 100576, https://doi.org/10.1016/j.apmt.2020.100576.

[15] P. Yılmaz, E. öztürk Er, S. Bakırdere, K. ülgen, B. özbek, Application of supercritical gel drying method on fabrication of mechanically improved and biologically safe three-component scaffold composed of graphene oxide/chitosan/hydroxyapatite and characterization studies, J. Mater. Res. Technol. 8 (2019) 5201–5216, https://doi.org/10.1016/j.jmrt.2019.08.043.

[16] Q. Wang, Y. Chu, J. He, W. Shao, Y. Zhou, K. Qi, L. Wang, S. Cui, A graded graphene oxide-hydroxyapatite/silk fibroin biomimetic scaffold for bone tissue engineering, Mater. Sci. Eng. C 80 (2017) 232–242, https://doi.org/10.1016/j.msec.2017.05.133.

[17] R. Al-Wafi, M.K. Ahmed, S.F. Mansour, Tuning the synthetic conditions of graphene oxide/magnetite/hydroxyapatite/cellulose acetate nanofibrous membranes for removing Cr(VI), Se(IV) and methylene blue from aqueous solutions, J. Water Process Eng. 38 (2020), 101543, https://doi.org/10.1016/j.jwpe.2020.101543.

[18] A.A. Francis, M.K. Abdel Rahman, The environmental sustainability of calcined calcium phosphates production from the milling of eggshell wastes and phosphoric acid, J. Clean. Prod. 137 (2016) 1432–1438, https://doi.org/10.1016/j.jclepro.2016.08.029.

[19] C. Daulbayev, F. Sultanov, A.V. Korobeinyk, M. Yeleuov, S. Azat, B. Bakbolat, A. Umirzakov, Z. Mansurov, Bio-waste-derived few-layered graphene/SrTiO3/PAN as efficient photocatalytic system for water splitting, Appl. Surf. Sci. 549 (2021), 149176, https://doi.org/10.1016/j.apsusc.2021.149176.

[20] M. Yeleuov, C. Seidl, T. Temirgaliyeva, A. Taurbekov, N. Prikhodko, B. Lesbayev, F. Sultanov, C. Daulbayev, S. Kumekov, Modified activated graphene-based carbon electrodes from rice husk for supercapacitor applications, Energies 13 (2020) 4943, https://doi.org/10.3390/en13184943.

[21] L. Ou, H. Wang, Z. Wu, P. Wang, L. Yang, X. Li, K. Sun, X. Zhu, R. Zhang, Effects of cadmium on osteoblast cell line: exportin 1 accumulation, p-JNK activation, DNA damage and cell apoptosis, Ecotoxicol. Environ. Saf. 208 (2021), 111668, https://doi.org/10.1016/j.ecoenv.2020.111668.

[22] S. Pang, Y. He, P. He, X. Luo, Z. Guo, H. Li, Fabrication of two distinct hydroxyapatite coatings and their effects on MC3T3-E1 cell behavior, Colloids Surf. B Biointerfaces 171 (2018) 40–48, https://doi.org/10.1016/j.colsurfb.2018.06.046.

[23] Y.C. Shin, J.H. Lee, O.S. Jin, S.H. Kang, S.W. Hong, B. Kim, J.C. Park, D.W. Han, Synergistic effects of reduced graphene oxide and hydroxyapatite on osteogenic differentiation of MC3T3-E1 preosteoblasts, Carbon 95 (2015) 1051–1060, https://doi.org/10.1016/j.carbon.2015.09.028.

[24] A.A. Menazea, M.K. Ahmed, Synthesis and antibacterial activity of graphene oxide decorated by silver and copper oxide nanoparticles, J. Mol. Struct. 1218 (2020), 128536, https://doi.org/10.1016/j.molstruc.2020.128536.

[25] J. McDonald-Wharry, M. Manley-Harris, K. Pickering, Carbonisation of biomass-derived chars and the thermal reduction of a graphene oxide sample studied using Raman spectroscopy, Carbon 59 (2013) 383–405, https://doi.org/10.1016/j.carbon.2013.03.033.

[26] H. Yarmand, S. Gharehkhani, S.F.S. Shirazi, A. Amiri, E. Montazer, H.K. Arzani, R. Sadri, M. Dahari, S.N. Kazi, Nanofluid based on activated hybrid of biomass carbon/graphene oxide: synthesis, thermo-physical and electrical properties, Int. Commun. Heat Mass Transf. 72 (2016) 10–15, https://doi.org/10.1016/j.icheatmasstransfer.2016.01.004.

[27] F. Chen, J. Yang, T. Bai, B. Long, X. Zhou, Facile synthesis of few-layer graphene from biomass waste and its application in lithium ion batteries, J. Electroanal. Chem. 768 (2016) 18–26, https://doi.org/10.1016/j.jelechem.2016.02.035.

[28] Y. Bleu, F. Bourquard, A.S. Loir, V. Barnier, F. Garrelie, C. Donnet, Raman study of the substrate influence on graphene synthesis using a solid carbon source via rapid thermal annealing, 50 (2019). 10.1002/jrs.5683.

[29] C. Li, Z. Zhuang, X. Jin, Z. Chen, A facile and green preparation of reduced graphene oxide using eucalyptus leaf extract, Appl. Surf. Sci. 422 (2017) 469–474, https://doi.org/10.1016/j.apsusc.2017.06.032.

[30] A.A. Yaqoob, A. Serrà, M.N.M. Ibrahim, A.S. Yaakop, Self-assembled oil palm biomass-derived modified graphene oxide anode: an efficient medium for energy transportation and bioremediating Cd (II) via microbial fuel cells, Arab. J. Chem. 14 (2021), 103121, https://doi.org/10.1016/j.arabjc.2021.103121.

[31] J. Klinkaewnarong, E. Swatsitang, C. Masingboon, S. Seraphin, S. Maensiri, Synthesis and characterization of nanocrystalline HAp powders prepared by using aloe vera plant extracted solution, Curr. Appl. Phys. 10 (2010) 521–525, https://doi.org/10.1016/j.cap.2009.07.014.

[32] R. Rodriguez, M. Estevez, S. Vargas, M. Gonzalez, R. Salazar, F. Pacheco, Synthesis and characterization of HAp-based porous materials, Mater. Lett. 63 (2009) 1558–1561, https://doi.org/10.1016/j.matlet.2009.04.019.

[33] M. González, U. Merino, S. Vargas, F. Quintanilla, R. Rodríguez, Synthesis and characterization of a HAp-based biomarker with controlled drug release for breast cancer, Mater. Sci. Eng. C 61 (2016) 801–808, https://doi.org/10.1016/j.msec.2016.01.015.

[34] S. Wang, F. Hu, J. Li, S. Zhang, M. Shen, M. Huang, X. Shi, Design of electrospun nanofibrous mats for osteogenic differentiation of mesenchymal stem cells, Nanomed. Nanotechnol. Biol. Med. 14 (2018) 2505–2520, https://doi.org/10.1016/j.nano.2016.12.024.

[35] H. Cheng, X. Yang, X. Che, M. Yang, G. Zhai, Biomedical application and controlled drug release of electrospun fibrous materials, Mater. Sci. Eng. C 90 (2018) 750–763, https://doi.org/10.1016/j.msec.2018.05.007.

[36] A. Chlanda, J. Rebis, E. Kijeńska, M.J. Wozniak, K. Rozniatowski, W. Swieszkowski, K.J. Kurzydlowski, Quantitative imaging of electrospun fibers by peakforce quantitative nanomechanics atomic force microscopy using etched scanning probes, Micron 72 (2015) 1–7, https://doi.org/10.1016/j.micron.2015.01.005.

[37] M.K. Ahmed, S.F. Mansour, R. Al-Wafi, A.A. Menazea, Composition and design of nanofibrous scaffolds of Mg/Se- hydroxyapatite/graphene oxide @ ε-polycaprolactone for wound healing applications, J. Mater. Res. Technol. 9 (2020) 7472–7485, https://doi.org/10.1016/j.jmrt.2020.04.094.

[38] G.W. Kwon, K.C. Gupta, K.H. Jung, I.K. Kang, Lamination of microfibrous PLGA fabric by electrospinning a layer of collagen-hydroxyapatite composite nanofibers for bone tissue engineering, Biomater. Res. 21 (2017) 11, https://doi.org/10.1186/s40824-017-0097-3.

[39] M. Wang, Z. Li, Y. Zhang, Y. Li, N. Li, D. Huang, B. Xu, Interaction with teichoic acids contributes to highly effective antibacterial activity of graphene oxide on gram-positive bacteria, J. Hazard. Mater. 412 (2021), 125333, https://doi.org/10.1016/j.jhazmat.2021.125333.

[40] S. Fathalipour, M. Mardi, Synthesis of silane ligand-modified graphene oxide and antibacterial activity of modified graphene-silver nanocomposite, Mater. Sci. Eng. C 79 (2017) 55–65, https://doi.org/10.1016/j.msec.2017.05.020.

[41] T. Pulingam, K.L. Thong, J.N. Appaturi, C.W. Lai, B.F. Leo, Mechanistic actions and contributing factors affecting the antibacterial property and cytotoxicity of graphene oxide, Chemosphere (2021), 130739, https://doi.org/10.1016/j.chemosphere.2021.130739.

[42] K.B. Narayanan, G.T. Park, S.S. Han, Antibacterial properties of starch-reduced graphene oxide–polyiodide nanocomposite, Food Chem. 342 (2021), 128385, https://doi.org/10.1016/j.foodchem.2020.128385.

[43] S. Prusty, K. Pal, D. Bera, A. Paul, M. Mukherjee, F. Khan, A. Dey, S. Das, Enhanced antibacterial activity of a novel biocompatible triarylmethane based ionic liquid-graphene oxide nanocomposite, Colloids Surf. B Biointerfaces 203 (2021), 111729, https://doi.org/10.1016/j.colsurfb.2021.111729.

[44] A.A. Menazea, M.K. Ahmed, Silver and copper oxide nanoparticles-decorated graphene oxide via pulsed laser ablation technique: preparation, characterization, and photoactivated antibacterial activity, Nano Struct. Nano Objects 22 (2020), 100464, https://doi.org/10.1016/j.nanoso.2020.100464.
[45] C.Y. Rao, X.Y. Sun, J.M. Ouyang, Effects of physical properties of nano-sized hydroxyapatite crystals on cellular toxicity in renal epithelial cells, Mater. Sci. Eng. C 103 (2019), 109807, https://doi.org/10.1016/j.msec.2019.109807.
[46] S. Morakul, Y. Otsuka, K. Ohnuma, M. Tagaya, S. Motozuka, Y. Miyashita, Y. Mutoh, Enhancement effect on antibacterial property of gray titania coating by plasma-sprayed hydroxyapatite-amino acid complexes during irradiation with visible light, Heliyon 5 (2019) e02207, https://doi.org/10.1016/j.heliyon.2019.e02207.
[47] M. Ramadas, G. Bharath, N. Ponpandian, A.M. Ballamurugan, Investigation on biophysical properties of hydroxyapatite/graphene oxide (HAp/GO) based binary nanocomposite for biomedical applications, Mater. Chem. Phys. 199 (2017) 179–184, https://doi.org/10.1016/j.matchemphys.2017.07.001.
[48] M. Yang, H. Liu, C. Qiu, I. Iatsunskyi, E. Coy, S. Moya, Z. Wang, W. Wu, X. Zhao, G. Wang, Electron transfer correlated antibacterial activity of biocompatible graphene nanosheets-TiO_2 coatings, Carbon 166 (2020) 350–360, https://doi.org/10.1016/j.carbon.2020.05.036.
[49] S. Huo, Y. Gao, L. Fang, Z. Jiang, Q. Xie, Q. Meng, G. Fei, S. Ding, Graphene oxide with acid-activated bacterial membrane anchoring for improving synergistic antibacterial performances, Appl. Surf. Sci. 551 (2021), 149444, https://doi.org/10.1016/j.apsusc.2021.149444.
[50] G. Cao, J. Yan, X. Ning, Q. Zhang, Q. Wu, L. Bi, Y. Zhang, Y. Han, J. Guo, Antibacterial and antibiofilm properties of graphene and its derivatives, Colloids Surf. B Biointerfaces 200 (2021), 111588, https://doi.org/10.1016/j.colsurfb.2021.111588.